Hepatitis C virus infection protein network.

B. de Chassey, V. Navratil, L. Tafforeau, M. S. Hiet, A. Aublin-Gex, S. Agaugué, G. Meiffren, F. Pradezynski, B. F. Faria, T. Chantier, et al.

HAL Id: pasteur-00456466

https://pasteur.hal.science/pasteur-00456466

Submitted on 15 Feb 2010

molecular
systems
biology

Hepatitis C virus infection protein network

B de Chassey[1,2,9], V Navratil[2,3,9], L Tafforeau[1,2,9], MS Hiet[1,2,10], A Aublin-Gex[1,2], S Agaugué[1,2,11], G Meiffren[1,2], F Pradezynski[1,2], BF Faria[1,2], T Chantier[1,2], M Le Breton[1,2], J Pellet[1,2], N Davoust[1,2], PE Mangeot[1,2], A Chaboud[2,4], F Penin[2,4], Y Jacob[5], PO Vidalain[6], M Vidal[7], P André[1,2,8], C Rabourdin-Combe[1,2] and V Lotteau[1,2,8],*

[1] IMAP Team, Inserm Unit 851, Lyon, France, [2] IFR128 BioSciences Lyon-Gerland, Université de Lyon, Lyon, France, [3] INRA UMR 754, rétrovirus et pathologie comparée, Lyon, France, [4] Institut de Biologie et Chimie des Protéines, CNRS UMR 5086, Lyon, France, [5] Unité Postulante de Génétique, Papillomavirus et Cancer Humain, Institut Pasteur, Paris, France, [6] Laboratoire de Génomique Virale et Vaccination, Institut Pasteur, CNRS URA 3015, Paris, France, [7] Center for Cancer Systems Biology, Dana-Farber Cancer Institute, Harvard Medical School, Boston, MA, USA and [8] Hospices Civils de Lyon, Hôpital de la Croix-Rousse, Laboratoire de virologie, Lyon, France
[9] These authors contributed equally to this work
[10] Present address: Department for Molecular Virology, University of Heidelberg, Heidelberg 69120, Germany.
[11] Present address: Service de Recherches en Hémato-Immunologie, CEA-DSV-DRM, Hôpital Saint-Louis, IUH, Paris 75475, France.
* Corresponding author. IMAP Team, Inserm Unit 851, 21, Av. T. Garnier, Lyon 69007, France. Tel.: +33 437 282 412; Fax: +33 437 282 341;
E-mail: vincent.lotteau@inserm.fr

A proteome-wide mapping of interactions between hepatitis C virus (HCV) and human proteins was performed to provide a comprehensive view of the cellular infection. A total of 314 protein–protein interactions between HCV and human proteins was identified by yeast two-hybrid and 170 by literature mining. Integration of this data set into a reconstructed human interactome showed that cellular proteins interacting with HCV are enriched in highly central and interconnected proteins. A global analysis on the basis of functional annotation highlighted the enrichment of cellular pathways targeted by HCV. A network of proteins associated with frequent clinical disorders of chronically infected patients was constructed by connecting the insulin, Jak/STAT and TGFβ pathways with cellular proteins targeted by HCV. CORE protein appeared as a major perturbator of this network. Focal adhesion was identified as a new function affected by HCV, mainly by NS3 and NS5A proteins.
Molecular Systems Biology 4 November 2008; doi:10.1038/msb.2008.66
Subject Categories: proteins; microbiology & pathogens
Keywords: functional analysis; hepatitis C; interactome; virus–host cell

Introduction

Hepatitis C virus (HCV) infection is characterized by a high rate of chronicity and concerns 170 millions of individuals worldwide. Chronically infected patients present liver injury essentially mediated by immune mechanisms and metabolic disorders associated with hepatic steatosis, fibrogenesis and insulin resistance to various extent (Negro, 2006; Moradpour *et al*, 2007). Long-term-infected patients have a high risk of developing cirrhosis and hepatocarcinoma, but despite considerable efforts, molecular basis of HCV pathology remains poorly understood. HCV genome is a positive-strand RNA of 9.6 kb encoding a polyprotein that is post-translationally processed into structural (CORE, E1, E2 and p7) and non-structural (NS2, NS3, NS4A, NS4B, NS5A and NS5B) proteins (Appel *et al*, 2006). HCV variants have been classified into six genotypes with biological and antigenic differences. Whereas infection by all genotypes is associated with insulin resistance and fibrosis, a correlation between hepatic steatosis severity

and viral replication is preferentially observed for genotype 3. Genotypic differences also correlate with interferon sensitivity, with genotypes 2 and 3 responding better to combined interferon and ribavirine therapy. We focused here on HCV genotype 1b, which is associated with insulin resistance, fibrosis, mild steatosis and poor sensitivity to treatment (Lonardo *et al*, 2004; Strader *et al*, 2004).

The rapidly growing knowledge of protein–protein interaction (PPI) networks (interactome) for human, model organisms and host–pathogen begins to provide network-based models for diseases. In a network approach, viral pathogenesis can be viewed as the expression of new constraints on the protein network imposed by the virus when connecting to the cellular interactome. Identification of topological and functional properties that are lost or deregulated, or that emerged in the 'infection network', becomes a major challenge for a systems understanding of viral infection (Tan *et al*, 2007).

High-throughput yeast two-hybrid (Y2H) screens of human cDNA library (Calderwood *et al*, 2007) and computation-based

analysis (Uetz *et al*, 2006) have been used previously to study Epstein–Barr virus (EBV), Kaposi sarcoma herpes virus and varicella zoster virus interactions with host cell factors. Analysis of virus–human protein inter-interactome network revealed that host interactors tend to be enriched in proteins that are highly connected in the cellular network (Calderwood *et al*, 2007; Dyer *et al*, 2008). These hub proteins are thought to be essential for the normal cell functioning and during pathogenesis.

Several laboratories have joined their efforts to develop infection mapping project (I-MAP). The goal of I-MAP is to provide a comprehensive view of viral infections at the protein level by mapping the interactions of a large number of viral proteins with host proteins. Screening and mapping have been designed to address specific questions, such as virulence/attenuation, species barrier, identification of therapeutic targets, chronicity and the risk of cancer development.

Here, a proteome-wide mapping approach of interactions between HCV and cellular proteins was performed to provide a comprehensive view of viral infection (Figure 1A). A viral ORFeome was first generated that included ORFs encoding all full-length mature proteins and several protein domains of genotype 1b strain (Supplementary Figure S1). These viral baits were screened against human cDNA libraries using a highly stringent Y2H assay (IMAP Y2H data set). Together with interactions extensively mined and curated from the literature (IMAP LCI data set), this comprehensive host–virus infection network was integrated into a reconstructed human protein–protein interactome. Analysis of the 'infection network' (V-H$_{HCV}$; Figure 1A) revealed topological features of cellular interactors and identified functional pathways related to viral biology and pathogenesis.

Results and discussion

Construction of an HCV–human interactome map

A comprehensive interactome map between HCV and cellular proteins was generated by Y2H screens. Twenty-seven constructs encoding full-length HCV mature proteins or discrete domains were cloned using a recombination-based cloning system (Walhout *et al*, 2000) (Supplementary Figure S1).
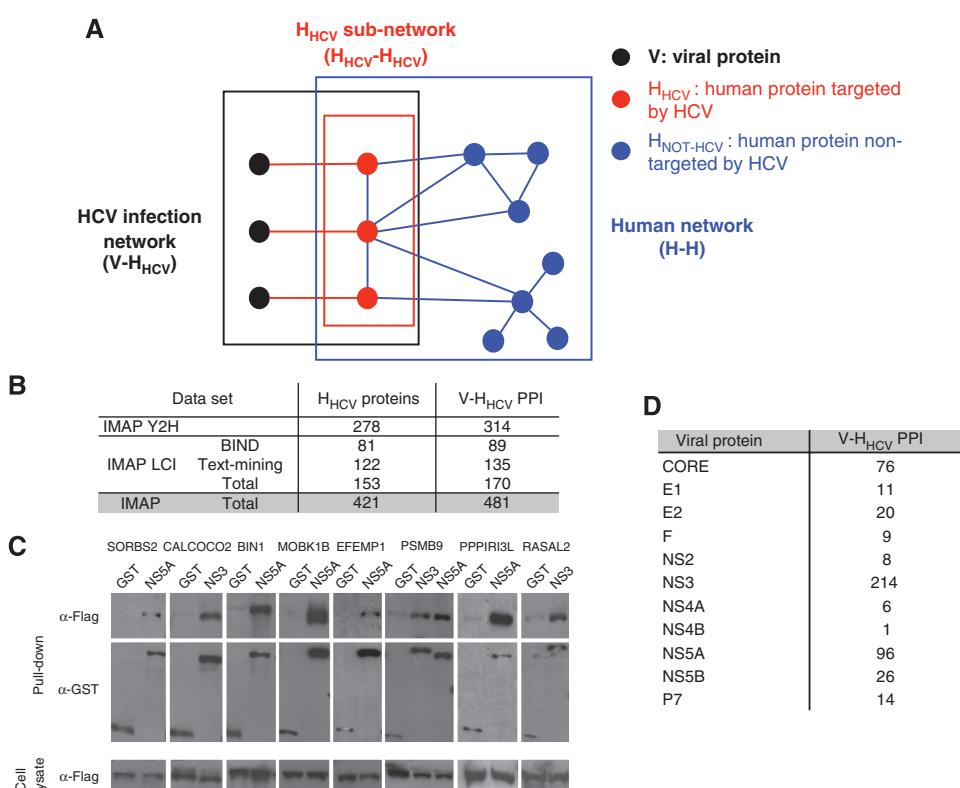

Figure 1 The HCV interaction network. (**A**) Nomenclature. V: viral protein (black node). H$_{HCV}$: human protein interacting with HCV proteins (red node). H$_{Not-HCV}$: human protein not interacting with HCV proteins (blue node). V-H$_{HCV}$: HCV–human protein interaction (red edge). H$_{HCV}$–H$_{HCV}$: interaction between HCV-interacting human proteins (blue edge). H–H: human–human protein interaction (blue edges). V-H$_{HCV}$ represents the interactions between HCV and human proteins (black box). H$_{HCV}$–H$_{HCV}$ is composed of human proteins interacting with viral proteins (red box). H–H network represents interactions between human proteins (blue box). (**B**) Number of proteins and interactions in HCV–human interaction network. Number of human proteins interacting with HCV proteins (H$_{HCV}$) and corresponding number of protein–protein interactions (V-H$_{HCV}$ PPI). Data are given for our yeast two-hybrid screens (IMAP Y2H) and for literature-curated interactions (IMAP LCI). (**C**) Validation of Y2H interactions by co-affinity purification assay. Nine out of 22 positive co-AP assays are shown, representing the following: NS5A-SORBS2, NS3-CALCOCO2, NS5A-BIN1, NS5A-MOBK1B, NS5A-EFEMP1, NS3-PSMB9 and NS5A-PSMB9, NS5A-PPPIRI3L, NS3-RASAL2. After pull-down with GST-tagged viral baits or with negative-control GST alone cellular preys are identified with anti-Flag antibody. Anti-GST antibody identifies either GST-alone or GST-tagged viral baits. Expression of cellular preys in cell lysate is controlled by anti-Flag (bottom panel). (**D**) Number of interactions by viral protein.

Four independent screens were performed with each HCV bait protein, probing two distinct human cDNA libraries, either by mating (IMAP1 screens) or by transformation (IMAP2 screens; see Materials and methods). Fetal brain and spleen cDNA libraries were used instead of a liver library because the liver is known to overexpress a large number of secreted proteins, which could interfere with the quality of the screens. Comparing EST data from fetal brain and spleen with EST data from liver revealed that 87% of genes expressed in the liver are also expressed in brain or spleen (http://www.ncbi.nlm.nih.gov/sites/entrez?db=unigene). A total of 314 HCV–human PPIs were identified, involving 278 human proteins (Figure 1B, IMAP Y2H data set in Supplementary Table SI). More than 90% of the cellular interactors identified are expressed in the liver. Pairwise interactions between HCV and human proteins were also extracted from the literature by automatic text mining and checked by expert curation (see Materials and methods; IMAP LCI data set in Supplementary Table SI). A total of 135 PPI were extracted from Pubmed and 89 were extracted from BIND database (Bader *et al*, 2003) (Figure 1B). The resulting HCV–human interactome is thus composed of 481 PPIs with 65% new interactions, involving 11 HCV proteins and 421 distinct human proteins (Figure 1B). IMAP1 and IMAP2 screens share 22 interactions (7% of IMAP Y2H data set). This overlap is in the range of previously reported data using two Y2H high-throughput screening methods (Lim *et al*, 2006) and suggests that despite screens characteristics, summarized in Supplementary Table SII, saturation has not been reached. Differences in the screening methods, such as sensitivity of the different yeast strains to selective drugs, differential growth rate of colonies and low penetrance of

interaction phenotype, could account for this observation. The low redundancy between IMAP Y2H and IMAP LCI data sets may also emphasize a high false-negative rate of the Y2H system, which would be in agreement with recent studies (Rual *et al*, 2005; Huang *et al*, 2007). An interesting hypothesis is that different methods of screening may lead to the exploration of different spaces of the HCV–human interactome. As false-positives may also contribute to the weak overlap of IMAP1 and IMAP2, two validation methods were used to assess the confidence of the IMAP Y2H data set. Two-thirds of the data set was retested by direct Y2H between viral protein baits and cellular protein preys identified by our Y2H screens (Y2H pairwise matrices). From the remaining interactions, 26 PPIs (25%) were retested by co-affinity purification and 22 PPIs could be validated (validation rate: 85%; Figure 1C and Supplementary Table SI). This Y2H data set was thus of very high confidence for further analysis at the topological and functional levels. In Table I, the top 21 new interactions validated by GST pull-down experiments and identified in one or two screens are shown. Analysis of the HCV-infection network (V-H$_{HCV}$, Figure 1A) showed that NS3, NS5A and CORE are the most connected proteins, with 214, 96 and 76 cellular partners, respectively, highlighting the potential multi-functionality of these proteins during infection (Supplementary Table SI, Figure 1D). Highly interacting proteins are known to be significantly more disordered than low-degree (LD) proteins (Haynes *et al*, 2006). Interestingly, NS3, NS5A and CORE are the only HCV proteins predicted to contain at least one intrinsic disordered region, according to DISOPRED2 (Ward *et al*, 2004) (prediction of protein disorder server; data not shown). This correlates well with the high degree (HD) of

Table I Top 21 HCV–human protein–protein interactions

HCV protein	Human gene name	Human protein official full name	Biological process
NS3	CALCOCO2	Calcium binding and coiled-coil domain 2	May have a function in viral life cycles
NS3	EIF4ENIF1	Eukaryotic translation initiation factor 4E nuclear import factor 1	Protein nuclear import
NS3	FRS3	Fibroblast growth factor receptor substrate 3	FGF receptor signalling pathway
NS3	CCDC21	Coiled-coil domain containing 21	Unknown
NS3	BCKDK	Branched-chain ketoacid dehydrogenase kinase	Branched-chain family amino-acid catabolic process
NS3	GBP2	Guanylate-binding protein 2, interferon-inducible	Immune response
NS3	KPNA1	Karyopherin alpha 1 (importin alpha 5)	NLS-bearing substrate import to the nucleus
NS3	PSMB9	Proteasome subunit, beta type, 9	Ubiquitin-dependent protein catabolic process
NS3	RASAL2	RAS protein activator-like 2	Regulation of small GTPase-mediated signal transduction
NS3	SMURF2	SMAD-specific E3 ubiquitin protein ligase 2	Regulation of TGFβ receptor signalling pathway
NS5A	EFEMP1	EGF-containing fibulin-like extracellular matrix protein 1	Integrity of fascia connective tissues
NS5A	GOLGA2	Golgi autoantigen, golgin subfamily a, 2	Vesicular transport
NS5A	GPS2	G protein pathway suppressor 2	JNK cascade
NS5A	ITGAL	Integrin, alpha L (antigen CD11A (p180), lymphocyte function-associated antigen 1; alpha polypeptide)	Integrin-mediated signalling pathway
NS5A	MOBK1B	MOB1, Mps one binder kinase activator-like 1B (yeast)	Cell cycle progression
NS5A	NAP1L2	Nucleosome assembly protein 1-like 2	Nucleosome assembly
NS5A	PPP1R13 L	Protein phosphatase 1, regulatory (inhibitor) subunit 13-like	Regulation of transcription, DNA-dependent
NS5A	PSMB9	Proteasome subunit, beta type, 9	Ubiquitin-dependent protein catabolic process
NS5A	SORBS2	Sorbin and SH3 domain containing 2	Cytoskeletal adaptor activity
NS5A	TXNDC11	Thioredoxin domain containing 11	Cell redox homeostasis
NS5A	VPS52	Vacuolar protein sorting 52 homolog (*S. cerevisiae*)	Vesicular transport

HCV proteins are referenced according to their NCBI mature peptide product name (column 1). Human proteins are referenced with their cognate NCBI gene name or their protein official full name with their main biological function (column 2, 3 and 4, respectively). The 21 interactions have been validated by GST pull-down. In the first three entries, interactions were identified in two screens. In the rest of the entries, interactions were identified in one screen. Interaction Bin1–NS5A has been removed from this list as already described in literature.
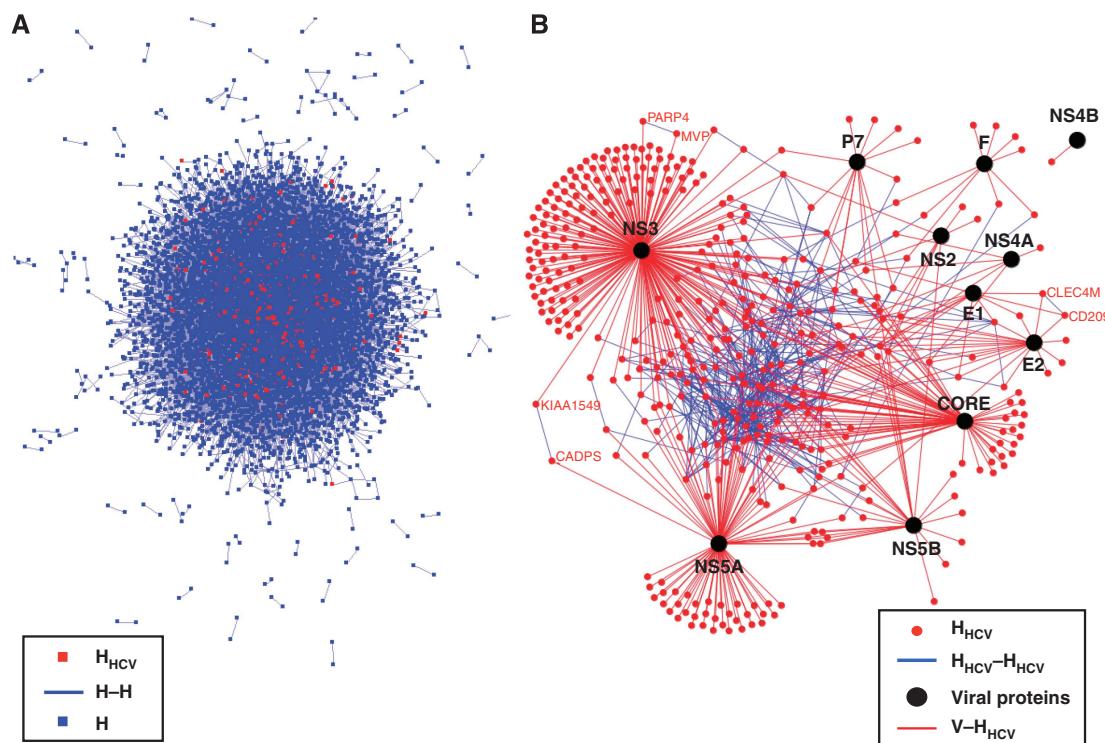
Figure 2 Graphical representation of the HCV–human interaction network. (**A**) Graphical representation of H–H network. Each node represents a protein and each edge represents an interaction. Red and blue nodes are H_{HCV} and $H_{Not-HCV}$, respectively. (**B**) Graphical representation of V–H_{HCV} interaction network. Black node: viral protein; red node: human protein; red edge: interaction between human and viral proteins (V–H_{HCV}); blue edge: interaction between human proteins (H_{HCV}–H_{HCV}). The largest component containing 196 proteins is represented in the middle of the network. Names of cellular proteins belonging to the three other connected components are also represented.

these proteins. In addition, 45 cellular proteins are targeted by more than one viral protein, suggesting their essentiality for virus biology (Calderwood *et al*, 2007) (Supplementary Table SIII).

A human PPI network (H–H network; Figure 1A) was reconstructed from eight databases (Gandhi *et al*, 2006) (see Materials and methods). This network is composed of 44 223 non-redundant PPIs between 9520 different proteins (Figure 2A, complete list of PPIs in Supplementary Table SIV), corresponding to 30% of the human proteome (the remaining proteins have no known cellular partners and can therefore not be included in this network). Interestingly, human proteins targeted by HCV (H_{HCV}) are clearly over-represented in this H–H network (IMAP Y2H data set: 76%; and IMAP LCI data set: 88%, exact Fisher test, *P*-value $< 2.2 \times 10^{-16}$). This suggests that HCV preferentially targets host proteins already known to be engaged in protein–protein interactions (Rual *et al*, 2005; Stelzl *et al*, 2005). For the IMAP LCI data set, the higher percentage of H_{HCV} integrated in the human interactome may be explained by inspection bias of well-studied proteins and biological pathways. Analysis of H_{HCV}–H_{HCV} subnetwork (all connected H_{HCV} proteins) showed that cellular proteins interacting with HCV are significantly more interconnected than expected for random subnetworks (Figures 1A and 2B, Supplementary methods). Indeed, the 338 H_{HCV} integrated into the human interactome are distributed into 131 connected components (versus 276 expected by random subnetworks; *z*-score-based test *P*-value $< 10^{-10}$,

Supplementary Table SV). The largest one is composed of 196 H_{HCV} (versus 18 expected by random subnetworks; *z*-test, *P*-value $< 10^{-10}$) and 127 are disconnected proteins. The three remaining connected components comprised two proteins. Two contained functionally related proteins (CLEC4M and CD209 are lectins involved in viral entry (Lozach *et al*, 2003); MVP and PARP4 are involved in Vault complex (Kedersha and Rome, 1986)) and one contained proteins not known to be functionally linked (KIAA1549 and CADPS).

Topological analysis of the HCV–human interaction network

To assess how HCV proteins interplay with the cellular protein network, we next focused on the centrality measures of H_{HCV} proteins integrated into the H–H interactome. Local (degree) and global (shortest path length and betweenness) centrality measures were calculated. Briefly, the degree (k) of a protein in a network corresponds to its number of direct partners and is therefore a measure of local centrality. Betweenness (b) is a global measure of centrality, as it measures the number of shortest paths (the minimum distance between two proteins in the network, l) that pass through a given protein. To provide an unbiased analysis, calculations were done on the basis of the 213 H_{HCV} from the IMAP Y2H data set integrated in the human interactome. The average degree, betweenness and shortest path length of the H–H network are 9.3, 1.6×10^{-4} and 4.04,

A

Data set	Proteins	ppi	k	b (10e−4)	l
H in H–H network	9520	44223	9.3	1.6	4.04
H_{HCV} in H–H network	213	72	15.6	3.8	3.50

C

B

Probability distribution (log–log scale)

Probability distribution (log–log scale)
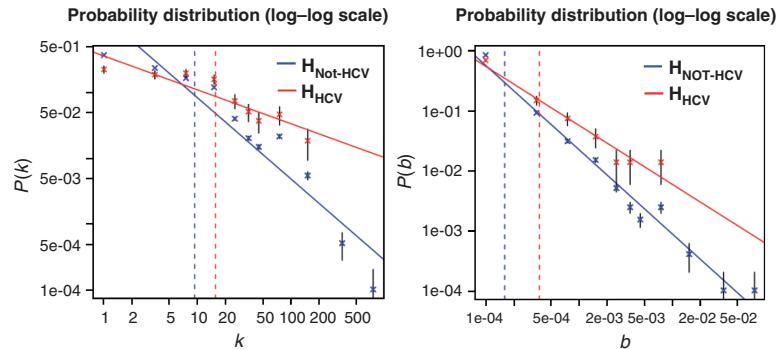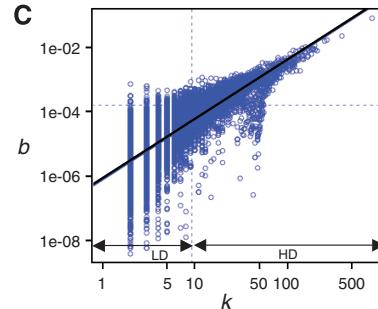
D
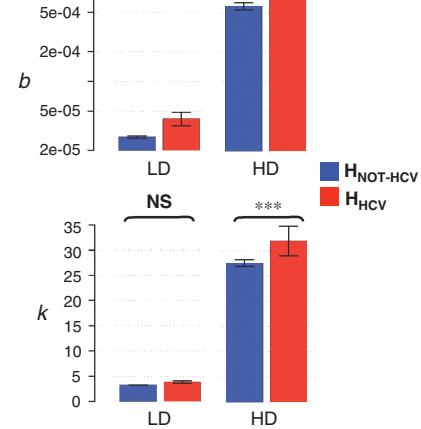
Figure 3 Topological analysis of the HCV–human interaction network. (**A**) Topological analysis of H and H_{HCV} in H–H network. Average values of degree (k), betweenness (b) and shortest path length (l) for all human proteins and for H_{HCV} from the IMAP Y2H data set. (**B**) Degree and betweenness distribution of H and H_{HCV} proteins in H–H network. $P(k)$ is the probability of a node to connect k other nodes in the network. $P(b)$ is the probability of a node to have a betweeness equal to b in the network. Normalized log degree (left) and log betweenness (right) distribution of H (blue) and H_{HCV} proteins (red). Solid line represents linear regression fit. Vertical dashed lines give mean degree and betweenness values. Each class is represented with conventional standard error. (**C**) Degree and betweenness correlation of H in H–H network. Normalized log degree (x axis) and log betweenness (y axis) of H proteins into H–H network. Black solid line represents the linear regression fit ($R^2 = 0.56$). Horizontal and vertical dashed lines give the mean degree and betweenness values, respectively. Low-degree (LD) and high-degree (HD) classes were defined by using the average degree cutoff. (**D**) Mean degree and betweenness of $H_{Not-HCV}$ and H_{HCV} for LD and HD proteins. Top: mean betweenness (log scale) of $H_{Not-HCV}$ (blue) and H_{HCV} (red) is given for LD and HD classes. Bottom: mean degree of $H_{Not-HCV}$ (blue) and H_{HCV} (red) is given for LD and HD classes. The conventional standard error threshold and the U-test P-value are represented (***P-value $< 10^{-10}$, NS: not significant).

respectively, which is in good agreement with previous reports (Ramirez *et al*, 2007) (Figure 3A). As the distribution of properties such as node degree and node betweenness in PPI networks appear to follow a power law, summarizing values by their distributions appears more appropriated for comparative analysis (Goh *et al*, 2002; Joy *et al*, 2005). The degree distribution of H_{HCV} and of the human interactome are significantly distinct (U-test P-value $< 10^{-3}$), with an average degree of H_{HCV} higher than the average degree of the human interactome (15.6 versus 9.3). The comparison of degree probability distribution reveals that H_{HCV} are preferentially represented in all class above the mean degree (Figure 3B, left). This indicates that HCV proteins have a strong tendency to interact with highly connected cellular proteins. However, as degree measures only local connectivity of proteins, global characteristics that could reflect information exchange and propagation in the network were investigated (Hernandez *et al*, 2007). At a global scale, the betweenness distribution of H_{HCV} and of the human interactome are significantly distinct (U-test P-value $< 10^{-3}$), with an average betweenness of H_{HCV} higher than the average betweenness of the human interactome (3.8×10^{-4} versus 1.6×10^{-4}). As for the degree, the

comparison of betweenness probability distribution shows an excess of H_{HCV} in all class above the mean betweenness (Figure 3B, right). In addition, the shortest path length distribution of H_{HCV} and of the human interactome were found significantly distinct (U-test P-value $< 10^{-5}$), with an average shortest path length of H_{HCV} lower than average shortest path length of the human interactome (3.50 versus 4.04) revealing the topological proximity of H_{HCV}. Both local and global centrality of H_{HCV} from the IMAP LCI data set were higher than for the IMAP Y2H data set, emphasizing the problem of literature inspection bias and reinforcing the unbiased approach of Y2H screening (Supplementary Table SV). To ensure that the preferential attachment to central H_{HCV} was not due to inherent bias associated to false positive in the H–H interactome, we performed the same analysis with a high-confidence, but less comprehensive, human interactome (Supplementary Table SV). This trend was maintained with this data set, confirming that H_{HCV} are highly central within the human interactome, both locally and globally, and appear relatively close to each other in this network. For comparative analysis of HCV and EBV, the centrality measures were also computed for H_{EBV} (data set from Calderwood *et al* (2007).

Table II KEGG pathway enrichment for H_{HCV}

KEGG name	CORE	E1	E2	NS3	NS5A	NS5B
Cell–cell and cell–ECM interactions						
Adherens junction	5			6 (5)		
Cell communication	6 (2)			8 (8)		
Cell adhesion molecules (CAMs)			3 (1)			
ECM–receptor interaction			2 (1)	6 (6)		
Focal adhesion				10 (9)	8 (2)	
Gap junction					4	
Tight junction						2
Signalling pathways						
TGFβ signalling pathway	4					
Jak-STAT signalling pathway	6				3	
Adipocytokine signalling pathway	5					
MAPK signalling pathway		3(2)				
Phosphatidylinositol signalling system			2		4	
Wnt signalling pathway				7 (3)		
Insulin signalling pathway					3	
B cell receptor receptor signalling pathway					3	
T cell receptor signalling pathway					5	

Over-represented KEGG pathways were identified after multiple testing adjustments (adjusted P-value $<5 \times 10^{-2}$) and are listed by viral protein. For each pathway, number of H_{HCV} is given, with the relative contribution of IMAP Y2H dataset in brackets. Shaded entries denote discussed pathways.

Degree, betweenness and shortest path followed the same tendency with H_{EBV} proteins (Supplementary Table SV and Supplementary Figure S2) and were in good agreement with a previous report (Calderwood *et al*, 2007). These results indicate that preferential attachment on central proteins may be a general hallmark of viral proteins as recently suggested by analysis of the literature (Dyer *et al*, 2008). The high centrality of proteins was previously shown to correlate with their functional essentiality for the yeast model organism (Jeong *et al*, 2001; Ekman *et al*, 2006). In mammals, lethal and disease-related proteins were found enriched in central proteins (Wachi *et al*, 2005; Stark *et al*, 2006; Goh *et al*, 2007; Hernandez *et al*, 2007). This suggests that HCV proteins interacted with essential proteins in the cell.

To determine which of the degree or the betweenness most influences the probability of interaction between viral and cellular proteins, we used a generalized linear model to test the separate and additive effects of both measures (Supplementary methods). This analysis revealed that betweenness better explains the probability of interaction between viral and human proteins (ANOVA P-value $<10^{-3}$). Figure 3C shows a partial correlation between k and b centrality measures ($R^2=56\%$, P-value $<10^{-16}$), explained by the high variability of betweenness at LD values. We thus asked whether this high variability observed at LD could explain the preponderant effect of betweenness. For this purpose, the data sets were split in LD and HD protein classes according to the average degree of the human interactome. For cellular proteins included in LD class, HCV interacts preferentially with proteins of high-betweenness independently of their degree property (Figure 3D). Within the HD class, interaction with HCV proteins is dependent on both betweenness and degree of cellular proteins. On the basis of a recent study in yeast (Joy *et al*, 2005), it can be extrapolated that LD high-betweenness H_{HCV} proteins could exert an effect as connectors or bottle-necks between cellular modules and may thus be essential for the infection.

Functional analysis of the HCV–human interaction network

To better understand biological functions targeted by HCV, we next tested the enrichment of specific pathways for all interactors of a given viral protein. This was done by analysing the H_{HCV} proteins with regard to the KEGG functional annotation pathways (Table II, Materials and methods). Although this approach is not totally unbiased because functions have not yet been attributed to all proteins, it remains a powerful way of incorporating conventional biology in system-level data sets. This analysis showed enrichment for three pathways associated with HCV clinical syndromes (insulin, TGFβ and Jak/STAT pathways) and identified focal adhesion as a novel pathway affected by HCV.

IJT network (insulin–Jak/STAT–TGFβ network)

Chronic infection by HCV is associated with an increased risk for metabolic disorders with the development of steatosis. Insulin resistance is a common feature of this process. It also contributes to liver fibrosis and is a predictor of a poor response to interferon-α (IFN-α) anti-viral therapy (D'Souza *et al*, 2005; Romero-Gomez *et al*, 2005). Conversely, IFN-α can prevent fibrosis progression (Poynard *et al*, 2002). TGFβ has a crucial function in maintaining cell growth and differentiation in the liver. It is a strong profibrogenic cytokine whose production is frequently enhanced during infection. Impaired TGFβ response is also observed during HCV infection (Schuppan *et al*, 2003). Although insulin, TGFβ and Jak/STAT pathways have been suspected to be involved in these clinical features (Romero-Gomez, 2006), their closely related perturbation during HCV infection remains largely unexplained. We thus used a network approach to identify cellular proteins targeted by HCV and localized at the interface of these pathways. The resulting interaction map was constructed to form the IJT network (insulin–Jak/STAT–TGFβ network,
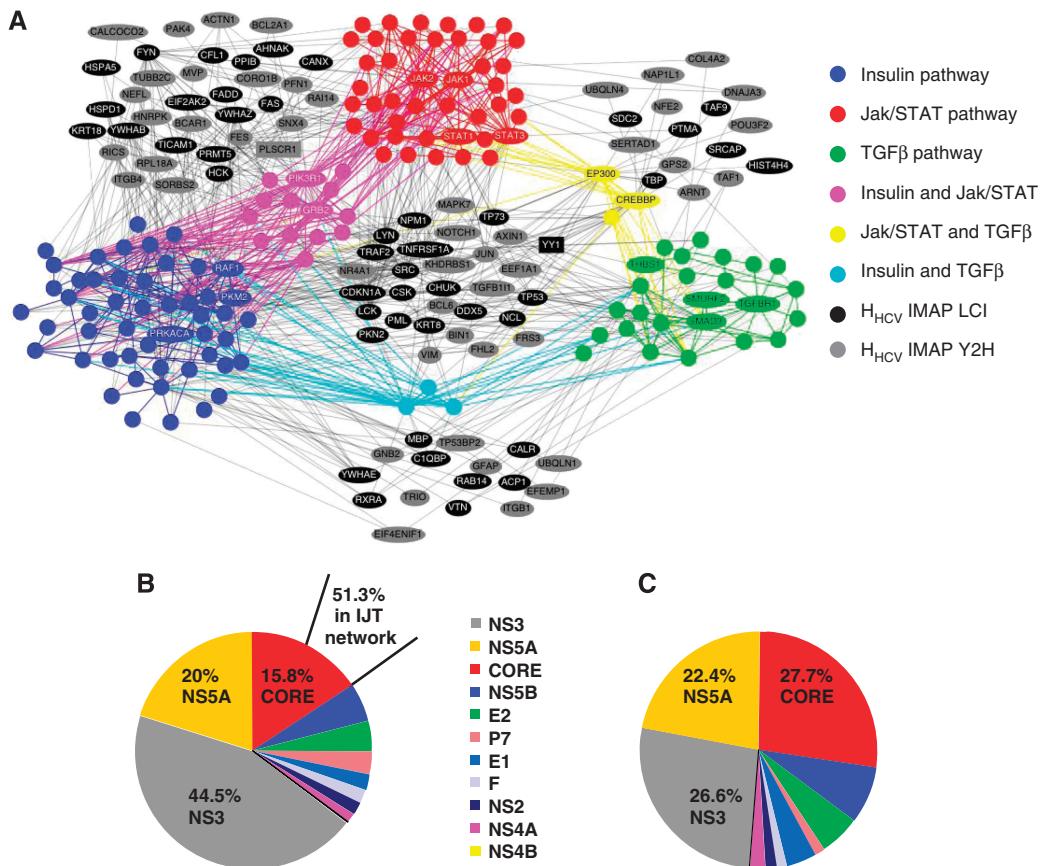
Figure 4 IJT network. (**A**) Graphical representation of IJT network. Protein (nodes) members of insulin (blue), Jak/STAT (red) and TGFβ (green) pathways according to KEGG annotation, and their interactions (edges) are shown (proteins interacting with HCV proteins are named). Proteins shared by two pathways are shown in secondary colours (pink, yellow and cyan). Grey and black nodes are neighbours that connect the KEGG pathways and that interact with HCV proteins (grey: protein from the IMAP Y2H data set; black: protein from the IMAP LCI data set). Neighbours interacting with HCV but not connecting the KEGG pathways are not represented. Discussed protein examples PLSCR1 and YY1 are in box. References to visualization tools are provided in supplementary files (network visualization). IJT network construction in Supplementary methods. (**B**) Relative contribution of each viral protein in V–H_{HCV}. Percentage interactions for the three most interacting viral proteins, relative to the total number of interactions as listed in Supplementary Table SI, are shown. A total of 51.3% of CORE interactions are concentrated in the IJT network. (**C**) Relative contribution of each viral protein in IJT network. Percentage interactions for the three most interacting viral proteins, relative to the total number of viral protein interactions with proteins of IJT network, are shown.

Figure 4A; Supplementary methods). Sixty-six H_{HCV} proteins are connecting two pathways, whereas 30 H_{HCV} proteins are connecting the three pathways. Interaction of these proteins with HCV proteins may thus induce functional perturbations that could expand to adjacent pathways. One of these proteins is PLSCR1 (Scramblase 1), connecting insulin and Jak/STAT pathways. Known to be involved in the redistribution of plasma membrane phospholipids (Sahu *et al*, 2007), this protein is also a potential activator of genes in response to interferon, and its knockdown with siRNA favours viral replication (Dong *et al*, 2004). Interestingly, PLSCR1$^{-/-}$ mice also exhibit an onset of insulin resistance (Wiedmer *et al*, 2004). Although not annotated in the insulin or Jak/STAT pathways, PLSCR1 thus appears essential for the functionality of these pathways. By interacting with PLSCR1, CORE could therefore interfere with both Jak/STAT and insulin pathways. Another example is the nuclear factor Yin Yang 1 (YY1), which exhibits a more central position in the IJT network as it connects the three pathways. HCV CORE interaction with YY1 has been previously shown to be functional relieving NPM1 expression. This observation could be extrapolated to PPARδ

expression and SMADs transcriptional activity in support of insulin and TGFβ pathway modulation (Kurisaki *et al*, 2003; Mai *et al*, 2006; He *et al*, 2008). Interestingly, BCL6, targeted by NS5A, is another transcriptional repressor at the interface of the three pathways that inhibit Smad signalling (Wang *et al*, 2008). It also exerts an effect as a corepressor of PPARδ (Lee *et al*, 2003) and it regulates the expression of a subset of Jak/STAT pathway target genes (Arbouzova *et al*, 2006). Thus, perturbation of these pathways can reasonably be expected as a consequence of BCL6 or YY1 targeting by HCV. Also central in the IJT network, NOTCH1 has been reported to interfere functionally with the three pathways. Literature analysis revealed that many of the proteins at the interface are actually known to have an important function in the regulation of one, two or the three pathways without being annotated in the KEGG database. These are only illustrative examples of cellular targets most likely to be involved in HCV-induced phenotypes. Although this molecular approach of the pathology is applicable to basal element of a system (proteins in this work) some of the clinical phenotypes observed in chronic HCV infection are most likely

to result from the integrative effect of protein interactions depicted in the IJT network. In addition, the robustness property of a network can confer its ability to remain functional in face of different perturbations despite the deregulation of a single protein.

Another issue that became apparent in the IJT network is that CORE protein mediates proportionally more interactions than the other HCV proteins (Figure 4B and C). Indeed, preferential interaction with IJT network was observed only with CORE (51.3%, Supplementary Table SVI). As a consequence, CORE makes 27.7% of the interactions in the IJT network, corresponding to a significant enrichment (exact Fisher test P-value $< 10^{-4}$). More precisely, this CORE's interactors are over-represented in Jak-STAT and TGFβ pathways (exact Fisher test P-value < 0.05) and in H_{HCV} connecting insulin–Jak/STAT and insulin–TGFβ pathways (exact Fisher test P-value < 0.05, Supplementary Table SVI). CORE thus appears as a major perturbator of the IJT network. Interestingly, transgenic mice expressing CORE develop insulin

resistance (Shintani *et al*, 2004; Pazienza *et al*, 2007). A proposed mechanism was that CORE-induced SOCS3 promotes proteasomal degradation of IRS1 and IRS2 through ubiquitination (Kawaguchi *et al*, 2004). As SOCS3 is also a negative regulator of Jak/STAT pathway, this could explain the occurrence of IFN-α resistance. Clearly, the IJT network indicates that the action of CORE is most likely to be much more complex that previously thought. Although the IJT network cannot yet be analysed dynamically, it remains that it provides a unique way of deciphering some of the complex disorders associated with chronicity. It is also worth considering that the IJT network may identify a series of genes involved in diseases, such as steatosis and fibrogenesis, in the absence of viral infection.

Focal adhesion

Focal adhesion was over-represented as a new function targeted by NS3 and NS5A proteins, with a major contribution
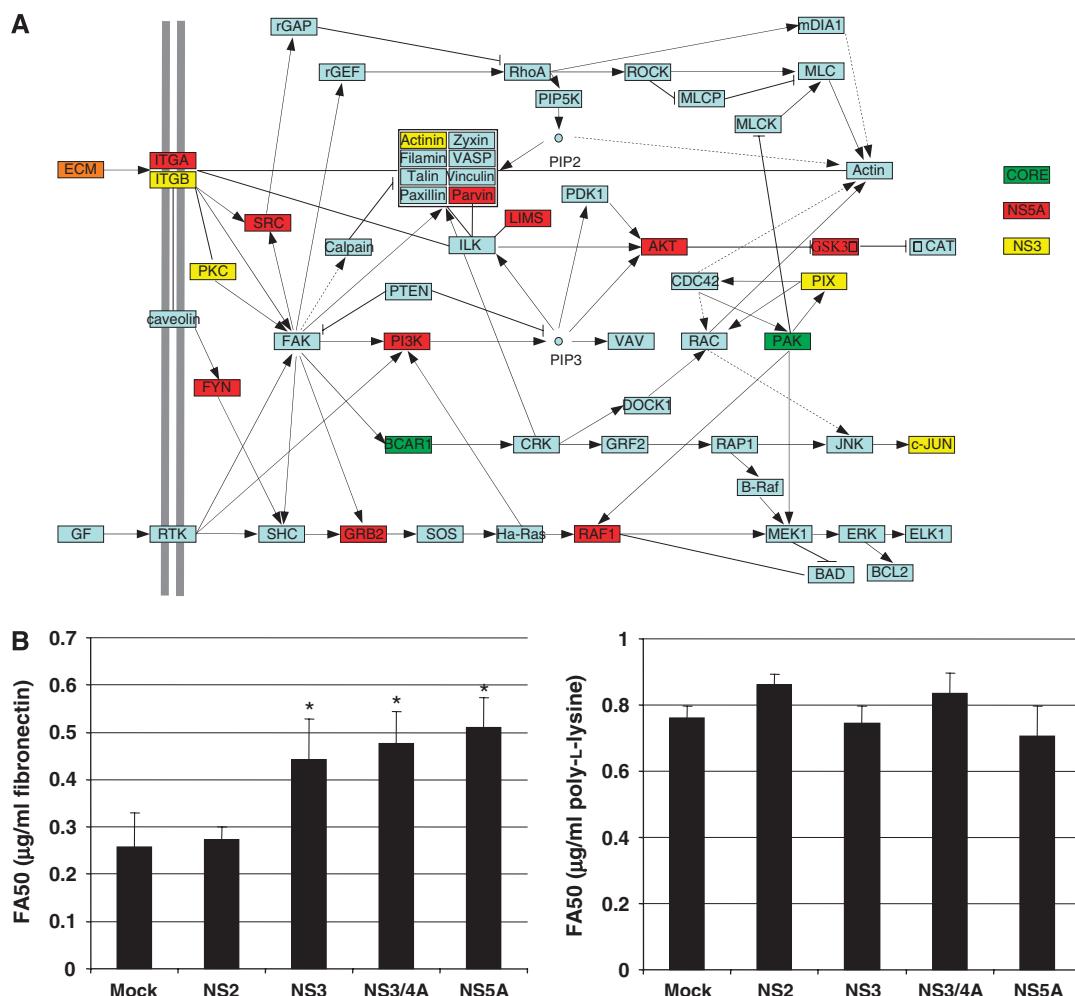

Figure 5 Interaction of HCV with focal adhesion. (**A**) Schematic representation of focal adhesion adapted from KEGG (ID: Hs04510). Proteins targeted by CORE, NS5A and NS3 HCV proteins are shown in yellow, red and green, respectively. ECM is a generic term for proteins of the extracellular matrix, some of which are targeted by HCV proteins (orange). (**B**) Functional validation of focal adhesion perturbation by NS3 and NS5A. Ninety-six-well plates were coated with fibronectin (left) or poly-L-lysine (right) at various concentrations. The 293T cells expressing NS2, NS3, NS3/4A or NS5A were plated on the matrix for 30 min. Adherent cells were stained with crystal violet. FA50 is the matrix concentration for half maximum adhesion. Values represent means of triplicate with standard deviation. *Student's *t*-test *P*-value < 0.05.

of data generated by IMAP Y2H screens (Table II). Integrin-linked focal adhesion complexes control cell adhesion to extracellular matrix (ECM) and association of these complexes with actin-cytoskeleton has an important function in cell migration. Upon binding to the ECM, both α and β integrin subunits recruit proteins establishing a physical link between the actin-cytoskeleton and signal transduction pathways. When deregulated, this functional process can lead to perturbation of cell mobility, detachment from the ECM and tumour initiation and progression. Figure 5A shows KEGG focal adhesion pathway with proteins targeted by HCV, mainly NS3 and NS5A proteins. Impact of single expression of NS3, NS3/4A or NS5A on focal adhesion functionality was assessed using a cellular adhesion assay on fibronectin and poly-L-lysine. These viral proteins significantly inhibited cell adhesion to fibronectin compared with NS2-expressing cells (an HCV protein with no interactor in the focal adhesion pathway) or mock-transfected cells, with 40% increase of FA50 (matrix concentration for half maximum adhesion) (Figure 5B left, Student's *t*-test *P*-value < 0.05). By contrast, adhesion to poly-L-lysine, which does not engage integrins, was not affected (Figure 5B right). The same inhibition level was observed for NS3/4A and NS3, suggesting that the enzyme activity of this protease does not have a major effect on focal adhesion perturbation. In addition to initiation and progression of cancer, the engagement of focal adhesion by HCV could have consequences on viral spreading. Interference with several steps of the actin-cytoskeleton remodelling has been described for retroviruses, which can exploit this process to surf along cellular protrusions of target cells to reach the entry site (Lehmann *et al*, 2005). It is conceivable that a related process, involving binding of the viral envelop to integrins, could be exploited by HCV to favour its transmission. This intriguing hypothesis will, however, be difficult to test until an efficient infection system of polarized cell is available.

Conclusion

In a network approach of HCV infection, the interaction map identifies all connections potentially needed for the virus to replicate and escape host defence. Whether all interactions really occur and have functional consequences is the open question of all interactome studies. The answer to this question necessitates the integration of system-level data sets of different origins that will set the stage for complex systems analysis of the infection. In a complex biological system, function cannot be predicted without understanding the component parts and their interactions and will result from the combination of theoretical knowledge of the cellular network with biological measurement of the interactions. Biological measurement, however, is still in the realm of low-throughput biology and needs major experimental improvement before prediction becomes the rule rather than the exception. Another fascinating challenge of this approach is to identify molecular signatures common to several viruses at the protein network level to develop original large-spectrum anti-viral molecules. A major step towards this goal is the high-throughput screening of a large variety of viruses, which is the aim of I-MAP.

Materials and methods

Construction of the HCV ORFeome

All HCV protein sequences were cloned in full length and domains except NS4B, for which no domain has been designed, using the euHCVdb facilities (http://euhcvdb.ibcp.fr; Combet *et al*, 2007) (Supplementary Figure S1). NS4A–NS3 fusion protein, as well as NS4A–NS3 protease domain were constructed (Kim *et al*, 1996; Taremi *et al*, 1998). All 27 ORFs from the HCV genotype 1b, isolate con1 (AJ238799) (Lohmann *et al*, 1999), were cloned in a Gateway recombinational cloning system (Walhout *et al*, 2000). Each ORF was PCR-amplified (with KOD polymerase, Novagen) using *attB1.1* and *attB2.1* recombination sites fused to forward and reverse primers, then cloned into pDONR223 (Rual *et al*, 2004). All entry clones were sequence-verified.

Yeast Two-hybrid (Y2H) screens

HCV ORFs were transferred from pDONR223 into bait vector (pPC97) to be expressed as Gal4–DB fusions in yeast. Two different screening methods were used (IMAP1 and IMAP2). For IMAP1, bait vectors were introduced in MAV203 yeast strain, and both human spleen and fetal brain AD-cDNA libraries (Invitrogen) were screened by transformation as described (Li *et al*, 2004). All primary positive clones (selected on SD−W−L−H+3−AT) were tested by further phenotypic assay using two additional reporter genes: *LacZ* (X-Gal colorimetric assay) and *URA3* (growth assay on 5-FOA supplemented medium). Positive clones that displayed at least two out of three positive phenotypes were retested in fresh yeasts: bait vectors were retransformed into MAV203 and each prey cDNA (obtained by colony PCR, see below) were transformed in combination with linearized prey vector (gap repair; Walhout and Vidal, 2001). Clones that did not retest were discarded. AD-cDNA were PCR-amplified and inserts were sequenced to identify interactors. IMAP2 screens were performed by yeast mating, using AH109 and Y187 yeast strains (Clontech; Albers *et al*, 2005). Bait vectors were transformed into AH109 (bait strain), and human spleen and fetal brain AD-cDNA libraries (Invitrogen) were transformed into Y187 (prey strain). Single bait strains were mated with prey strain, then diploids were plated on SD−W−L−H+3−AT medium. Positive clones were maintained onto this selective medium for 15 days to eliminate any contaminant AD-cDNA plasmid (Vidalain *et al*, 2004). AD-cDNAs were PCR-amplified and inserts were sequenced.

Text-mining of interactions between HCV and human proteins

Literature-curated interactions (LCI), describing binary interactions between cellular and HCV proteins, were extracted from BIND database and PubMed (publications before August 2007) by using an automatic text-mining pipeline completed by expert curation process. For the text-mining approach, all abstracts related to 'HCV' and 'protein interactions' keywords were retrieved, subjected to a sentencizer (sentence partition) and a part-of-speech tagger for gene name (based on NCBI gene name and aliases) and interaction verbs (Rebholz-Schuhmann *et al*, 2008) (interact, bind, attach and so on). Sentences presenting co-occurrences of at least one human gene name, one viral gene name and one interaction term were prioritized to curation by human expert.

Validation by co-affinity purification

Cellular ORFs (interacting domains found in Y2H screens) were cloned by recombinational cloning from a pool of human cDNA library or the MGC cDNA plasmids using KOD polymerase (Toyobo) into pDONR207 (Invitrogen). After validation by sequencing, these ORFs were transferred into pCi-neo-3× FLAG gateway-converted. HCV ORFs were transferred into pDEST27 (GST fusion in N-term). A total of 4×10^5 HEK-293T cells were then co-transfected (6 μl JetPei, Polyplus) with 1.5 μg of each pair of plasmid. Controls are GST-alone against 3× FLAG-tagged prey. Two days after transfection, cells were

harvested and lysed (0.5% NP-40, 20 mM Tris–HCl (pH 8.0), 180 mM NaCl, 1 mM EDTA and Roche complete protease inhibitor cocktail). Cell lysates were cleared by centrifugation for 20 min at 13 000 r.p.m. at 4°C and soluble protein complexes were purified by incubating 300 μg of cleared cell lysate with 40 μl glutathione sepharose 4B beads (GE Healthcare). Beads were then washed extensively with lysis buffer and proteins were separated on SDS–PAGE and transferred to nitrocellulose membrane. A total of 50 μg of cleared cell lysate was analysed by western blot to check the amount of 3 × FLAG-tagged cell protein. GST-tagged viral proteins and 3 × FLAG-tagged cellular proteins were detected using standard immunoblotting techniques using anti-GST (Covance) and anti-FLAG M2 (Sigma) monoclonal antibodies.

Integrated human interactome network (H–H network)

Only physical and direct binary protein-protein interactions were retrieved from BIND (Bader *et al*, 2003), BioGRID (Stark *et al*, 2006), DIP (Xenarios *et al*, 2002), GeneRIF (Lu *et al*, 2007), HPRD (Peri *et al*, 2004), IntAct (Kerrien *et al*, 2007), MINT (Chatr-aryamontri *et al*, 2007) and Reactome (Vastrik *et al*, 2007). NCBI official gene names were used to unify protein ACC, protein ID, gene name, symbol or alias defined in different genome reference databases (i.e ENSEMBL, UNIPROT, NCBI, INTACT, HPRD and so on) and to eliminate interaction redundancy due to the existence of different protein isoforms for a single gene. Thus, the gene name was used in the text to identify the proteins. Finally, only non-redundant protein–protein interactions were retained for building the human interactome data set.

Topological analysis

The R (http://www.r-project.org/) statistical environment was used to perform statistical analysis and the igraph R package (http://cneurocvs.rmki.kfki.hu/igraph/) to compute network connected components, centrality (degree, betweenness) and shortest path measures.

The Wilcoxon–Mann–Whitney rank sum test (the *U*-test) was chosen to statistically challenge observed differences. The *U*-test is a non-parametric alternative to the paired Student's *t*-test for the case of two related samples or repeated measurements on a single sample. The generalized linear model and ANOVA analysis was used to respectively model and test the separate and additive effects of degree and betweenness on the probability that HCV proteins interact with human proteins.

Functional analysis using KEGG annotations

Cellular pathway data were retrieved from KEGG (Aoki-Kinoshita and Kanehisa, 2007) and the Kyoto Encyclopedia of Genes and Genomes (http://www.genome.jp/kegg/) and were used to annotate NCBI gene functions. For each viral–host protein interactors, the enrichment of specific KEGG pathway was tested by using an exact Fisher test (*P*-value $< 5 \ 10^{-2}$) followed by the Benjamini and Hochberg multiple test correction (Benjamini *et al*, 2001) to control false discovery rate.

Cell-adhesion assay

Serial dilutions (from 20 to 0.04 μg/ml) of fibronectin or poly-L-lysine in PBS were coated on 96-well microplates overnight at 4°C. Non-specific binding sites were saturated at room temperature with PBS 1% BSA for 1 h. HEK 293T cells were transfected with pCi-neo-3 × FLAG NS2, NS3, NS3/4A or NS5A (JetPei, Polyplus), collected 2 days later with 2 mM EDTA in PBS, spread in triplicate at 1×10^5 cell per well in serum-free medium with 0.1% BSA and incubated for 30 min at 37°C. Non-adherent cells were washed away and adherent cells were fixed with 3.7% paraformaldehyde. Cells were stained with 0.5% crystal violet in 20% methanol for 20 min at room temperature and washed five times in H_2O. Staining was extracted from 50% ethanol in 50 mM sodium citrate, pH 4.5, and the absorbance was read at 590 nm on an ELISA reader (MRX microplate reader, Dynatech Laboratories). Values were normalized to 100% adhesion at 10 μg/ml. The percentage of adhesion was determined for each cell type at each matrix concentration. 50% of maximum adhesions (FA50) were calculated from the curves (Supplementary Figure S3) (adapted from Miao *et al*, 2000).

Supplementary information

Supplementary information is available at the *Molecular Systems Biology* website (www.nature.com/msb).

Conflict of interest

The authors declare that they have no conflict of interest.

References

Albers M, Kranz H, Kober I, Kaiser C, Klink M, Suckow J, Kern R, Koegl M (2005) Automated yeast two-hybrid screening for nuclear receptor-interacting proteins. *Mol Cell Proteomics* **4:** 205–213

Aoki-Kinoshita KF, Kanehisa M (2007) Gene annotation and pathway mapping in KEGG. *Methods Mol Biol* **396:** 71–92

Appel N, Schaller T, Penin F, Bartenschlager R (2006) From structure to function: new insights into hepatitis C virus RNA replication. *J Biol Chem* **281:** 9833–9836

Arbouzova NI, Bach EA, Zeidler MP (2006) Ken & barbie selectively regulates the expression of a subset of Jak/STAT pathway target genes. *Curr Biol* **16:** 80–88

Bader GD, Betel D, Hogue CW (2003) BIND: the Biomolecular Interaction Network Database. *Nucleic Acids Res* **31:** 248–250

Benjamini Y, Drai D, Elmer G, Kafkafi N, Golani I (2001) Controlling the false discovery rate in behavior genetics research. *Behav Brain Res* **125:** 279–284

Calderwood MA, Venkatesan K, Xing L, Chase MR, Vazquez A, Holthaus AM, Ewence AE, Li N, Hirozane-Kishikawa T, Hill DE, Vidal M, Kieff E, Johannsen E (2007) Epstein–Barr virus and virus human protein interaction maps. *Proc Natl Acad Sci USA* **104:** 7606–7611

Chatr-aryamontri A, Ceol A, Palazzi LM, Nardelli G, Schneider MV, Castagnoli L, Cesareni G (2007) MINT: the Molecular INTeraction database. *Nucleic Acids Res* **35:** D572–D574

Combet C, Garnier N, Charavay C, Grando D, Crisan D, Lopez J, Dehne-Garcia A, Geourjon C, Bettler E, Hulo C, Le Mercier P, Bartenschlager R, Diepolder H, Moradpour D, Pawlotsky JM, Rice CM, Trepo C, Penin F, Deleage G (2007) euHCVdb: the European hepatitis C virus database. *Nucleic Acids Res* **35:** D363–D366

D'Souza R, Sabin CA, Foster GR (2005) Insulin resistance plays a significant role in liver fibrosis in chronic hepatitis C and in the response to antiviral therapy. *Am J Gastroenterol* **100:** 1509–1515

Dong B, Zhou Q, Zhao J, Zhou A, Harty RN, Bose S, Banerjee A, Slee R, Guenther J, Williams BR, Wiedmer T, Sims PJ, Silverman RH (2004) Phospholipid scramblase 1 potentiates the antiviral activity of interferon. *J Virol* **78:** 8983–8993

Dyer MD, Murali TM, Sobral BW (2008) The landscape of human proteins interacting with viruses and other pathogens. *PLoS Pathog* **4:** e32

Ekman D, Light S, Bjorklund AK, Elofsson A (2006) What properties characterize the hub proteins of the protein-protein interaction network of *Saccharomyces cerevisiae*? *Genome Biol* **7:** R45

Gandhi TK, Zhong J, Mathivanan S, Karthick L, Chandrika KN, Mohan SS, Sharma S, Pinkert S, Nagaraju S, Periaswamy B, Mishra G, Nandakumar K, Shen B, Deshpande N, Nayak R, Sarker M, Boeke JD, Parmigiani G, Schultz J, Bader JS *et al* (2006) Analysis of the human protein interactome and comparison with yeast, worm and fly interaction datasets. *Nat Genet* **38:** 285–293

Goh KI, Cusick ME, Valle D, Childs B, Vidal M, Barabasi AL (2007) The human disease network. *Proc Natl Acad Sci USA* **104:** 8685–8690

Goh KI, Oh E, Jeong H, Kahng B, Kim D (2002) Classification of scale-free networks. *Proc Natl Acad Sci USA* **99:** 12583–12588

Haynes C, Oldfield CJ, Ji F, Klitgord N, Cusick ME, Radivojac P, Uversky VN, Vidal M, Iakoucheva LM (2006) Intrinsic disorder is a common feature of hub proteins from four eukaryotic interactomes. *PLoS Comput Biol* **2:** e100

He CQ, Ding NZ, Fan W (2008) YY1 repressing peroxisome proliferator-activated receptor delta promoter. *Mol Cell Biochem* **308:** 247–252

Hernandez P, Huerta-Cepas J, Montaner D, Al-Shahrour F, Valls J, Gomez L, Capella G, Dopazo J, Pujana MA (2007) Evidence for systems-level molecular mechanisms of tumorigenesis. *BMC Genomics* **8:** 185

Huang H, Jedynak BM, Bader JS (2007) Where have all the interactions gone? Estimating the coverage of two-hybrid protein interaction maps. *PLoS Comput Biol* **3:** e214

Jeong H, Mason SP, Barabasi AL, Oltvai ZN (2001) Lethality and centrality in protein networks. *Nature* **411:** 41–42

Joy MP, Brock A, Ingber DE, Huang S (2005) High-betweenness proteins in the yeast protein interaction network. *J Biomed Biotechnol* **2005:** 96–103

Kawaguchi T, Yoshida T, Harada M, Hisamoto T, Nagao Y, Ide T, Taniguchi E, Kumemura H, Hanada S, Maeyama M, Baba S, Koga H, Kumashiro R, Ueno T, Ogata H, Yoshimura A, Sata M (2004) Hepatitis C virus down-regulates insulin receptor substrates 1 and 2 through up-regulation of suppressor of cytokine signaling 3. *Am J Pathol* **165:** 1499–1508

Kedersha NL, Rome LH (1986) Isolation and characterization of a novel ribonucleoprotein particle: large structures contain a single species of small RNA. *J Cell Biol* **103:** 699–709

Kerrien S, Alam-Faruque Y, Aranda B, Bancarz I, Bridge A, Derow C, Dimmer E, Feuermann M, Friedrichsen A, Huntley R, Kohler C, Khadake J, Leroy C, Liban A, Lieftink C, Montecchi-Palazzi L, Orchard S, Risse J, Robbe K, Roechert B (2007) IntAct—open source resource for molecular interaction data. *Nucleic Acids Res* **35:** D561–D565

Kim JL, Morgenstern KA, Lin C, Fox T, Dwyer MD, Landro JA, Chambers SP, Markland W, Lepre CA, O'Malley ET, Harbeson SL, Rice CM, Murcko MA, Caron PR, Thomson JA (1996) Crystal structure of the hepatitis C virus NS3 protease domain complexed with a synthetic NS4A cofactor peptide. *Cell* **87:** 343–355

Kurisaki A, Kurisaki A, Valcourt U, Terentiev AA, Pardali K, Ten Dijke P, Heldin CH, Ericsson J, Moustakas A (2003) Nuclear factor YY1 inhibits transforming growth factor beta- and bone morphogenetic protein-induced cell differentiation. *Mol Cell Biol* **23:** 4494–4510

Lee CH, Chawla A, Urbiztondo N, Liao D, Boisvert WA, Evans RM, Curtiss LK (2003) Transcriptional repression of atherogenic inflammation: modulation by PPARdelta. *Science* **302:** 453–457

Lehmann MJ, Sherer NM, Marks CB, Pypaert M, Mothes W (2005) Actin- and myosin-driven movement of viruses along filopodia precedes their entry into cells. *J Cell Biol* **170:** 317–325

Li S, Armstrong CM, Bertin N, Ge H, Milstein S, Boxem M, Vidalain PO, Han JD, Chesneau A, Hao T, Goldberg DS, Li N, Martinez M, Rual JF, Lamesch P, Xu L, Tewari M, Wong SL, Zhang LV, Berriz GF (2004) A map of the interactome network of the metazoan *C. elegans*. *Science* **303:** 540–543

Lim J, Hao T, Shaw C, Patel AJ, Szabo G, Rual JF, Fisk CJ, Li N, Smolyar A, Hill DE, Barabasi AL, Vidal M, Zoghbi HY (2006) A protein–protein interaction network for human inherited ataxias and disorders of Purkinje cell degeneration. *Cell* **125:** 801–814

Lohmann V, Korner F, Koch J, Herian U, Theilmann L, Bartenschlager R (1999) Replication of subgenomic hepatitis C virus RNAs in a hepatoma cell line. *Science* **285:** 110–113

Lonardo A, Adinolfi LE, Loria P, Carulli N, Ruggiero G, Day CP (2004) Steatosis and hepatitis C virus: mechanisms and significance for hepatic and extrahepatic disease. *Gastroenterology* **126:** 586–597

Lozach PY, Lortat-Jacob H, de Lacroix de Lavalette A, Staropoli I, Foung S, Amara A, Houles C, Fieschi F, Schwartz O, Virelizier JL, Arenzana-Seisdedos F, Altmeyer R (2003) DC-SIGN and L-SIGN are high affinity binding receptors for hepatitis C virus glycoprotein E2. *J Biol Chem* **278:** 20358–20366

Lu Z, Cohen KB, Hunter L (2007) GeneRIF quality assurance as summary revision. *Pac Symp Biocomput* 269–280

Mai RT, Yeh TS, Kao CF, Sun SK, Huang HH, Wu Lee YH (2006) Hepatitis C virus core protein recruits nucleolar phosphoprotein B23 and coactivator p300 to relieve the repression effect of transcriptional factor YY1 on B23 gene expression. *Oncogene* **25:** 448–462

Miao H, Burnett E, Kinch M, Simon E, Wang B (2000) Activation of EphA2 kinase suppresses integrin function and causes focal-adhesion-kinase dephosphorylation. *Nat Cell Biol* **2:** 62–69

Moradpour D, Penin F, Rice CM (2007) Replication of hepatitis C virus. *Nat Rev Microbiol* **5:** 453–463

Negro F (2006) Insulin resistance and HCV: will new knowledge modify clinical management? *J Hepatol* **45:** 514–519

Pazienza V, Clement S, Pugnale P, Conzelman S, Foti M, Mangia A, Negro F (2007) The hepatitis C virus core protein of genotypes 3a and 1b downregulates insulin receptor substrate 1 through genotype-specific mechanisms. *Hepatology* **45:** 1164–1171

Peri S, Navarro JD, Kristiansen TZ, Amanchy R, Surendranath V, Muthusamy B, Gandhi TK, Chandrika KN, Deshpande N, Suresh S, Rashmi BP, Shanker K, Padma N, Niranjan V, Harsha HC, Talreja N, Vrushabendra BM, Ramya MA, Yatish AJ, Joy M (2004) Human protein reference database as a discovery resource for proteomics. *Nucleic Acids Res* **32:** D497–D501

Poynard T, McHutchison J, Manns M, Trepo C, Lindsay K, Goodman Z, Ling MH, Albrecht J (2002) Impact of pegylated interferon alfa-2b and ribavirin on liver fibrosis in patients with chronic hepatitis C. *Gastroenterology* **122:** 1303–1313

Ramirez F, Schlicker A, Assenov Y, Lengauer T, Albrecht M (2007) Computational analysis of human protein interaction networks. *Proteomics* **7:** 2541–2552

Rebholz-Schuhmann D, Arregui M, Gaudan S, Kirsch H, Jimeno A (2008) Text processing through Web services: calling whatizit. *Bioinformatics* **24:** 296–298

Romero-Gomez M (2006) Insulin resistance and hepatitis C. *World J Gastroenterol* **12:** 7075–7080

Romero-Gomez M, Del Mar Viloria M, Andrade RJ, Salmeron J, Diago M, Fernandez-Rodriguez CM, Corpas R, Cruz M, Grande L, Vazquez L, Munoz-De-Rueda P, Lopez-Serrano P, Gila A, Gutierrez ML, Perez C, Ruiz-Extremera A, Suarez E, Castillo J (2005) Insulin resistance impairs sustained response rate to peginterferon plus ribavirin in chronic hepatitis C patients. *Gastroenterology* **128:** 636–641

Rual JF, Hirozane-Kishikawa T, Hao T, Bertin N, Li S, Dricot A, Li N, Rosenberg J, Lamesch P, Vidalain PO, Clingingsmith TR, Hartley JL, Esposito D, Cheo D, Moore T, Simmons B, Sequerra R, Bosak S, Doucette-Stamm L, Le Peuch C (2004) Human ORFeome version 1.1: a platform for reverse proteomics. *Genome Res* **14:** 2128–2135

Rual JF, Venkatesan K, Hao T, Hirozane-Kishikawa T, Dricot A, Li N, Berriz GF, Gibbons FD, Dreze M, Ayivi-Guedehoussou N, Klitgord N, Simon C, Boxem M, Milstein S, Rosenberg J, Goldberg DS, Zhang LV, Wong SL, Franklin G (2005) Towards a proteome-scale map of the human protein–protein interaction network. *Nature* **437:** 1173–1178

Sahu SK, Gummadi SN, Manoj N, Aradhyam GK (2007) Phospholipid scramblases: an overview. *Arch Biochem Biophys* **462:** 103–114

Schuppan D, Krebs A, Bauer M, Hahn EG (2003) Hepatitis C and liver fibrosis. *Cell Death Differ* **10**(Suppl 1)**:** S59–S67

Shintani Y, Fujie H, Miyoshi H, Tsutsumi T, Tsukamoto K, Kimura S, Moriya K, Koike K (2004) Hepatitis C virus infection and diabetes: direct involvement of the virus in the development of insulin resistance. *Gastroenterology* **126:** 840–848

Stark C, Breitkreutz BJ, Reguly T, Boucher L, Breitkreutz A, Tyers M (2006) BioGRID: a general repository for interaction datasets. *Nucleic Acids Res* **34:** D535–D539

Stelzl U, Worm U, Lalowski M, Haenig C, Brembeck FH, Goehler H, Stroedicke M, Zenkner M, Schoenherr A, Koeppen S, Timm J, Mintzlaff S, Abraham C, Bock N, Kietzmann S, Goedde A, Toksoz E, Droege A, Krobitsch S, Korn B (2005) A human protein-protein interaction network: a resource for annotating the proteome. *Cell* **122:** 957–968

Strader DB, Wright T, Thomas DL, Seeff LB (2004) Diagnosis, management, and treatment of hepatitis C. *Hepatology* **39:** 1147–1171

Tan SL, Ganji G, Paeper B, Proll S, Katze MG (2007) Systems biology and the host response to viral infection. *Nat Biotechnol* **25:** 1383–1389

Taremi SS, Beyer B, Maher M, Yao N, Prosise W, Weber PC, Malcolm BA (1998) Construction, expression, and characterization of a novel fully activated recombinant single-chain hepatitis C virus protease. *Protein Sci* **7:** 2143–2149

Uetz P, Dong YA, Zeretzke C, Atzler C, Baiker A, Berger B, Rajagopala SV, Roupelieva M, Rose D, Fossum E, Haas J (2006) Herpesviral protein networks and their interaction with the human proteome. *Science* **311:** 239–242

Vastrik I, D'Eustachio P, Schmidt E, Joshi-Tope G, Gopinath G, Croft D, de Bono B, Gillespie M, Jassal B, Lewis S, Matthews L, Wu G, Birney E, Stein L (2007) Reactome: a knowledge base of biologic pathways and processes. *Genome Biol* **8:** R39

Vidalain PO, Boxem M, Ge H, Li S, Vidal M (2004) Increasing specificity in high-throughput yeast two-hybrid experiments. *Methods* **32:** 363–370

Wachi S, Yoneda K, Wu R (2005) Interactome-transcriptome analysis reveals the high centrality of genes differentially expressed in lung cancer tissues. *Bioinformatics* **21:** 4205–4208

Walhout AJ, Temple GF, Brasch MA, Hartley JL, Lorson MA, van den Heuvel S, Vidal M (2000) GATEWAY recombinational cloning: application to the cloning of large numbers of open reading frames or ORFeomes. *Methods Enzymol* **328:** 575–592

Walhout AJ, Vidal M (2001) High-throughput yeast two-hybrid assays for large-scale protein interaction mapping. *Methods* **24:** 297–306

Wang D, Long J, Dai F, Liang M, Feng XH, Lin X (2008) BCL6 represses Smad signaling in transforming growth factor-beta resistance. *Cancer Res* **68:** 783–789

Ward JJ, McGuffin LJ, Bryson K, Buxton BF, Jones DT (2004) The DISOPRED server for the prediction of protein disorder. *Bioinformatics* **20:** 2138–2139

Wiedmer T, Zhao J, Li L, Zhou Q, Hevener A, Olefsky JM, Curtiss LK, Sims PJ (2004) Adiposity, dyslipidemia, and insulin resistance in mice with targeted deletion of phospholipid scramblase 3 (PLSCR3). *Proc Natl Acad Sci USA* **101:** 13296–13301

Xenarios I, Salwinski L, Duan XJ, Higney P, Kim SM, Eisenberg D (2002) DIP, the Database of Interacting Proteins: a research tool for studying cellular networks of protein interactions. *Nucleic Acids Res* **30:** 303–305